engineering proceedings

MDPI

Proceeding Paper

Interreg Plastron: Reuse of Marine Plastic Through Additive Manufacturing †

Alessandro Seitone [1,*], Adrianna Bardelli [2], Pedro Lopez-Merino [3], Matilde Minuto [1], Massimiliano Avalle [1], Maila Castellano [2,*], Christophe Charlier [3], Eric Guerci [3], Stefano Becherini [4] and Mattia Frascio [1,*]

[1] Dipartimento di Ingegneria Meccanica, Energetica e dei Trassporti, Università degli Studi di Genova, Via All'opera Pia 15A, 16145 Genova, Italy
[2] Dipartimento di Chimica e Chimica Industriale, Università degli Studi di Genova, Via Dodecaneso 31, 16146 Genova, Italy
[3] Groupe de Recherche en Droit, Économie et Gestion (GREDEG), Université Côte d'Azur/CNRS, 250 rue Albert Einstein, 06560 Valbonne, France
[4] Revet S.p.A., Viale America, 104-56025 Pontedera, Italy; stefano.becherini@revet.com
* Correspondence: alessandro.seitone@gmail.com (A.S.); maila.castellano@unige.it (M.C.); mattia.frascio@edu.unige.it (M.F.)
† Presented at the 54th Conference of the Italian Scientific Society of Mechanical Engineering Design (AIAS 2025), Florence, Italy, 3–6 September 2025.

Abstract

The PLASTRON (Reuse of plastic from the sea using additive manufacturing as a strategy for the challenges of tourism supply chains and business resilience (Italian acronym: *riuso della PLAstica dal mare usando la manifattura additiva come Strategia per le sfide delle filiere del TuRismO e la resilieNza delle imprese*)) project aims to enhance the sustainability of coastal communities by improving plastic waste management and fostering the transition to efficient circular economy models, aligned with the European Green Deal. A Franco-Italian multidisciplinary team is testing low-investment local initiatives for collecting plastics from coasts, ports, and the sea. The project develops protocols to integrate waste into the recycling chain and create value-added goods through additive manufacturing. Special focus is given to degraded marine litter and mixed plastics, exploring their reuse via blending with other materials and natural additives. The focus was on the characterisation of two material blends, polyolefin mix (MPO) and Polyethylene terephthalate (PET), both with plastic marine litter. The processability of the MPO blend was comparable to that of commercial recycled MPO. The differences observed between 3D printing and injection moulding for the MPO derived from marine litter were negligible, unlike those found in the commercial MPO. The PET, modified with 0.8% chain extender additive, exhibited performance equivalent to—or in some cases even superior to—that of virgin commercial PET. However, 3D printing processing induced a certain brittleness in the material.

Keywords: circular economy; recycling of plastic sea; 3D printing; small communities; economic valorisation

Check for updates

Academic Editors: Nicola Bonora, Umberto Galietti, Luigi Bruno, Davide Castagnetti, Cristiana Del Prete, Mario Guagliano and Vigilio Fontanari

Published: 1 April 2026

Copyright: © 2026 by the authors. Licensee MDPI, Basel, Switzerland. This article is an open access article distributed under the terms and conditions of the Creative Commons Attribution (CC BY) license.

1. Introduction

The dispersion of plastics into the sea represents one of the main global environmental emergencies: only a minimal share of the plastics produced is recycled, while most end up in landfills, are incinerated, or leak into the environment [1]. A significant portion of mismanaged waste reaches the seas through waterways, with severe impacts on marine

and coastal ecosystems. Plastics are the predominant component of marine litter (60–90%), originating mainly from land-based sources [2,3].

Managing this plastic waste is complex: prolonged exposure to sunlight, saltwater, and weathering degrades its properties, making recovery and industrial reuse difficult. Moreover, the areas most affected are often islands or coastal regions with limited infrastructure and strong seasonal tourist flows, where collection and treatment costs are high. In this context, decentralised, community-based approaches that rely on accessible technologies can transform the waste problem into opportunities for the circular economy, local employment, and innovation [4,5].

It is within this framework that the European Interreg 2024–2027 Plastron Project was launched, addressing in an interdisciplinary way the challenges of recovering and valorising plastics dispersed in the marine environment. The project involves the municipalities of Stintino (Sardinia, Italy) and Île Rousse (Corse, France) as pilot sites, the University of Genoa (Liguria, Italy) and Cispel Toscana with its subsidiary Revet S.p.A. (Toscana, Italy) for technical development, and benefits from the evaluation of sustainable economic models carried out by the Université Côte d'Azur (Côte d'Azur, France).

The main objective is to develop innovative proximity-based solutions, with particular focus on the use of marine plastics in additive manufacturing technologies. Plastron also investigates the mechanical recycling of marine plastics, especially polyolefin mix (MPO)—Polypropylene (PP), High-density polyethylene (HDPE), Low-density polyethylene (LDPE), and Polyethylene terephthalate (PET), which account for much of marine litter [6,7].

The PLASTRON project aims to transform these often heterogeneous and degraded materials into plastic granules suitable for Fused Granulate Additive Manufacturing (FGF).

Fused Granulate Additive Manufacturing (FGAM) is an advanced 3D printing technique that uses thermoplastic materials in granular form—often recycled plastic pellets—instead of traditional filaments or resins. In FGAM, the granules are fed into a heated extruder, melted, and deposited layer by layer to build objects [8]. Unlike conventional fused filament fabrication (FFF), FGAM does not require strict dimensional tolerance, making the process more cost-effective and sustainable [9–13].

FGAM enables large-format printing, offers flexibility in material selection, and supports closed-loop recycling, as printed objects can be regranulated and reprinted [14]. It aligns with the principles of eco-design, promoting modularity, repairability, and reduced resource consumption, thus representing a key technology for transforming plastic waste into durable, customisable, and environmentally responsible solutions [15].

To improve the granulated materials mechanical properties, the use of additives and fibres is considered: in addition to traditional mineral fillers (talc, carbonates), Plastron explores more sustainable solutions such as local organic waste (eggshells, residues from the wine, olive oil, and rice industries) and lignocellulosic additives derived from agricultural biomass as also explored in other studies [16–18].

The raw materials studied come from:

- plastics collected through marine cleanup campaigns,
- organic waste and agricultural by-products from the project regions.

Extrusion and mechanical recycling tests were carried out on plastics collected along the Tuscan and Ligurian coasts. After regranulation, the materials were processed by injection moulding and 3D printing to produce specimens for tensile and flexural tests. The results were compared with reference materials: the Refill 33K polyolefin mix from Revet S.p.A. for the MPO study, and V-PET and R-PET values reported in the literature for PET analysis.

The overarching goal of PLASTRON is to generate a circular economy model that can be replicated in other sites (namely, coastal areas exposed to plastic pollution) and

contribute with technical solutions that can be scaled to encompass larger regions. Circular economy principles aim to redesign systems so that materials like plastic remain in the production loop through reuse, recycling, and redesign, rather than leaking into nature [19]. Our method thus seeks to establish a circular value chain, where collected waste is cleaned, processed into granules, and reused to produce functional products—such as replacement parts for the fishing industry—or design-oriented objects [20,21]. We therefore combine environmental protection, technological innovation, and sustainable development of coastal and island communities.

This article focuses on the technical aspects of the project. Work coordinated by Université Côte d'Azur delves more into the socio-economic aspects of the model [22].

2. Materials and Methods Introduction

In this work, studies were carried out on polyolefin mixtures MPO and PET, which were separately granulated. For the MPO, the addition of fillers, antioxidants, and compatibilisers was considered. For PET, the effect of different concentrations of a chain extender, specifically Joncryl ADR-4400 (Lithlon, Shanghai, China), was evaluated.

2.1. Materials

Collection took place during five cleanup interventions conducted along the coastal areas of Tuscany and Liguria, specifically in the municipalities of Genoa, Sturla, Zoagli, Lerici, Marina di Pisa, and Marina di Vecchiano (Figure 1a). Approximately 25 kg of plastic waste was recovered with cleanup interventions, consisting of about 50% PET and 50% MPO (Figure 1b). The operations covered both emerged areas (beaches and rocky shores) and the first 20 m of seabed along the shoreline, and were carried out by divers and volunteers. In addition, 2 kg of plastic material were retrieved at depths between 300 and 400 m by fishermen (Figure 1c). During fishing activities in the waters of Rapallo and Santa Margherita Ligure (Italy).



Figure 1. (**a**) Collection zone; (**b**) Superficial plastic marine litter; (**c**) Underwater plastic marine litter.

The collected material was first sorted to separate the fractions of interest and subsequently rinsed in cold water, with bottles opened and sand and stones removed. It was then processed using a CMG G17-38-3K-ARK grinder (CMG Granulators S.p.a., Budrio (BO), Italy), equipped with a super-tangential cutting system with three movable knives, two fixed knives, and a 20 mm perforated screen. The grinding process produced flakes ranging from 10 to 30 mm in size.

The flakes were then washed in an industrial Electrolux LVA 100 vegetable washer (Electrolux Professional S.p.A., Pordenone (PN), Italy) featuring a 5 × 5 mm perforated basket and a 6 L capacity, using cold water and a non-foaming detergent. For heavily

encrusted material, typically from the seabed, the use of a citric acid mixture was explored. After washing, the material was centrifuged at 250 rpm to remove excess water and subsequently dried in an Argolab 50 L oven (Giorgio Bormac s.r.l., Carpi (MO), Italy) at 50 °C for 24 h for MPO and 80 °C for 24 h for PET. Following drying, the material underwent a second grinding using the CMG grinder equipped with a 4 mm screen, thoroughly cleaned after the first grinding cycle (Figure 2).

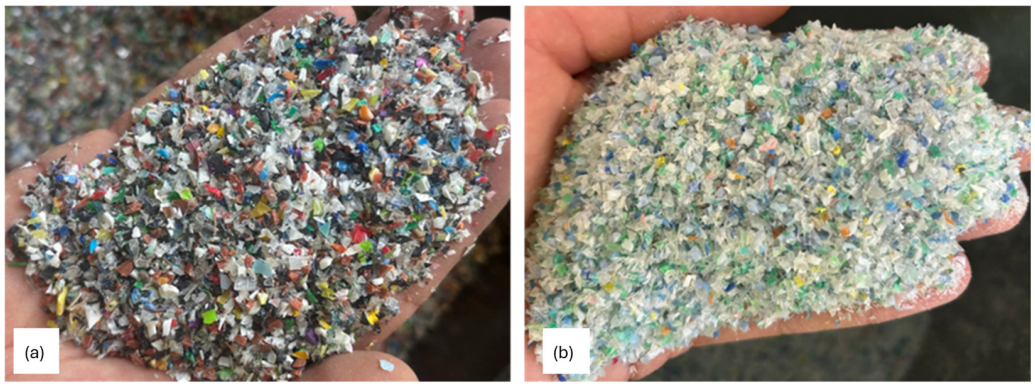


Figure 2. (**a**) PP/PE Flakes; (**b**) PET Flakes.

Since a filtration system downstream of the extrusion screw was not available, impurity removal was entirely ensured during the pretreatment stage. This step is essential to prevent contamination during subsequent melting and extrusion processes, improving interlayer adhesion in 3D printing.

2.2. Extrusion and Granulation of the Material

To ensure the highest material quality during extrusion, the obtained flakes were subjected to dehumidification prior to melting using a New Omap WDC.E15 MT-30 30-L desiccant dryer (New Omap S.r.l., Casalserugo (PD), Italy), in order to reduce residual moisture to optimal levels. The drying cycles are 160 °C for 12 h for PET and 80° for 2 h for MPO [23].

The material was subsequently extruded using a Eur.ex.ma X-TWIN S-40 D co-rotating twin-screw extruder (EUR.EX.MA—Eurotech Extrusion Machinery Srl, Tradate (VA), Italy) (Figure 3a) equipped with 22 mm diameter screws and an L/D ratio of 40:1, ensuring intensive mixing. Temperature control throughout the process was achieved via eight heating zones, each equipped with a water-cooling system. To remove moisture and degradation gases, two degassing zones were employed: one atmospheric and one under high vacuum.

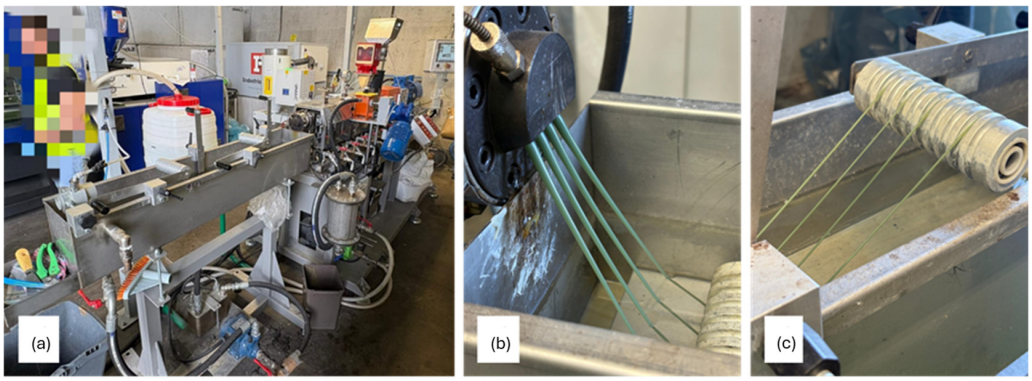


Figure 3. (**a**) Extrusion line; (**b**) Four holes die (**c**) Water cooling system.

For material dosing, the main volumetric feeder with a single screw was used for the ground material, while a lateral volumetric system was employed for the addition of additives, pigments, and powders. Filament extrusion was carried out through a die with four 4 mm holes (Figure 3b), allowing the extrusion of coarse materials with pellet sizes ranging from 2 to 3 mm. MPO-based materials were processed by extrusion in the range of 185–200 °C, while PET-based materials were processed in the range of 250–270 °C [23]. For pelletising, a dry system was used, featuring a closed-circuit cooling bath (Figure 3c) and a rotary cutting system. The wet filament was dried using compressed air.

PP and PE were extruded together with the addition of 1 wt% antioxidant to prevent oxidative degradation at the high processing temperatures. A total of 8 kg of polyolefin blend MPO (75% PE–25% PP) was obtained. Specifically, Basf Irganox B215 (BASF SE, Ludwigshafen, Germany), a synergistic long-term thermal stabiliser mixture of Irgafos 168 and Irganox 1010, was used [24].

From the resulting MPO Tal Quale M1, 5 kg were taken to produce two mixtures: MPO TQ_M2, containing 10 wt% eggshell powder as a carbonate substitute [25], and MPO TQ_M3, containing 10 wt% olive pit powder and 1 wt% compatibiliser (BASF Epolene E43). The size of the filler powder provided by AgroMateriae (AgroMateriae srl, Faenza (RA), Italy) is 14 µm for ESF B1—Eggshell powder and 25-50 µm for OSF B1—Olive Stone powder [26] (Figure 4).

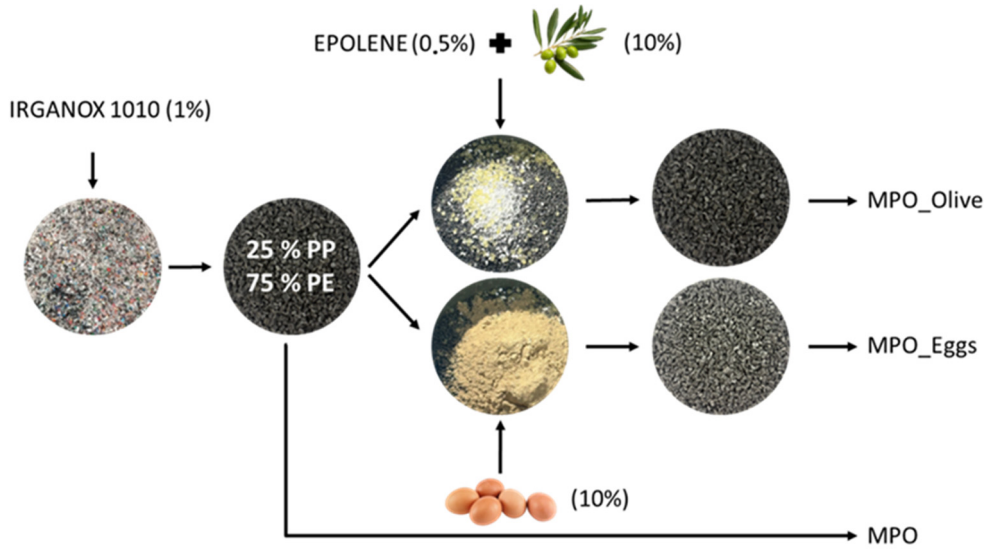


Figure 4. MPO Extrusion Flowchart.

PET, on the other hand, was extruded without the addition of fillers but was modified with a chain extender (BASF Joncryl® ADR-4400, BASF SE, Ludwigshafen, Germany) at increasing mass fractions of 0.8%, 1%, and 1.5%.

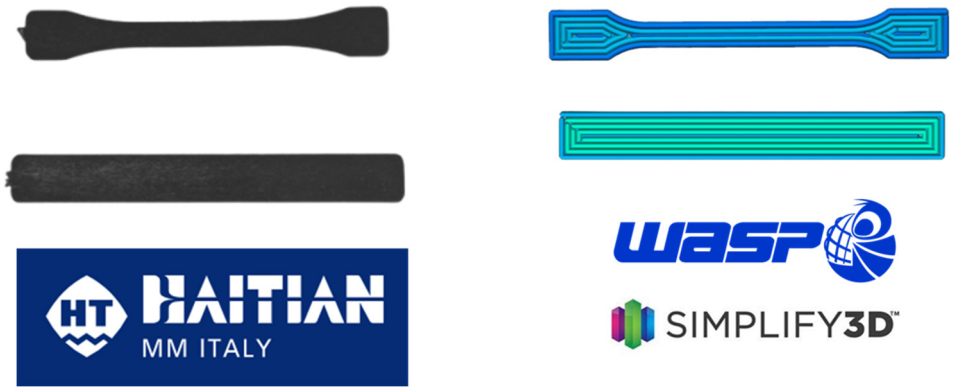
Images of the cross-section of the granules were obtained using a Nikon SMZ800 stereomicroscope (Nikon Europe, Amstelveen, The Netherlands).

2.3. Mechanical Testing

The recovered materials were subjected to mechanical characterisation tests. Tensile and flexural strength tests were performed using an Instron 34SC-2 single-column materials Testing System, Force Capacity 2 kN. Tensile tests were conducted in accordance with ISO 527-2:2025 Plastics, Determination of tensile properties Part 2: Test conditions for moulding and extrusion plastics, using type 1BA specimens. In contrast, flexural tests were conducted in accordance with ISO 178:2019 Plastics, Determination of flexural properties, using rectangular samples with cross dimensions of 10.0 ± 0.2 mm width, 4.0 ± 0.2 mm thickness, and 80 ± 2 mm length.

Type 1BA specimens were selected instead of type 1A due to the limited amount of material available for testing, with the understanding that the results are less representative compared to the standard type 1A specimens, but still acceptable for describing the mechanical properties of the material, as permitted by the standard. In accordance with ISO 527-2 and ISO 178, between three and five specimens per material were tested, starting with an initial crosshead speed of 1 mm/min to determine the elastic modulus. The speed was subsequently increased to 50 mm/min for highly deformable materials and to 5 mm/min for stiffer materials, up to final fracture. Three-point bending tests were carried out at a crosshead speed of 2 mm/min with a support span of 80 mm, using five replicates per material.

Specimens (Figure 5a) were produced by injection moulding using a Haitian MARS 900 III injection moulding machine (Ningbo, China, Haitian Plastics Machinery), with processing parameters reported in Table 1.



(**a**) (**b**)

Figure 5. (**a**) Injection Moulding Samples (**b**) Additive Manufacturing Samples.

Table 1. Injection moulding parameters.

Injection Moulding Parameters			
/	MPO	PET	U.M
Channel Temperature	210	280	°C
Pressure	40	500	bar
Maintenance Time	7	8	s
Mould Temperature	32	32	°C
Conditioning	48	48	h/T. Amb.

Additionally, specimens were fabricated via additive manufacturing using a WASP 4070 HDP 3D printer equipped with a 1 mm nozzle (WASP S.r.l., Massa Lombarda (RA), Italy), employing a rectilinear infill pattern at 0° (Figure 5b), with slicing parameters set in Simplify3D.

WASP 4070 HDP is a printer based on FGAM (Fused Additive Manufacturing) technology, equipped with an HDP screw extruder with two heating zones (Barrel and Nozzle) (Figure 6). The granular feedstock was supplied via compressed air from a non-insulated, non-sealed metal hopper mounted on the machine. The printer is equipped with a temperature-controlled chamber and a polypropylene build plate with vacuum fixation.



Figure 6. WASP 4070 HDP.

The printing of the specimens allowed for a visual assessment of the most common material behaviours, such as interlayer adhesion, warping, and shrinkage, thereby helping to identify the optimal printing conditions. Prior to processing, the material was dehumidified in a dryer for 12 h at 160 °C [27].

The additive manufacturing parameters identified and adopted for the printing of PET and MPO specimens are reported in Table 2. Before each 3D printing test, the materials are deeply dried in the New Omap desiccant dryer to avoid hydrolytic degradation processes during the extrusion.

Table 2. Additive Manufacturing parameters.

	MPO	MPO_Eggs	MPO_Olive	PET 0.8	PET 1	PET 1.5	U.M.
Nozzle Diameter	1	1	1	-	1	-	mm
Barrel Temperature	130	130	130	-	240	-	°C
Nozzle Temperature	240	240	240	-	260	-	°C
Plate Temperature	50	50	50	-	80	-	°C
Camera Temperature	20	20	20	-	20	-	°C
Cooling Fan	30	30	30	-	0	-	%
Extrusion Speed	30	30	30	-	40	-	mm/s

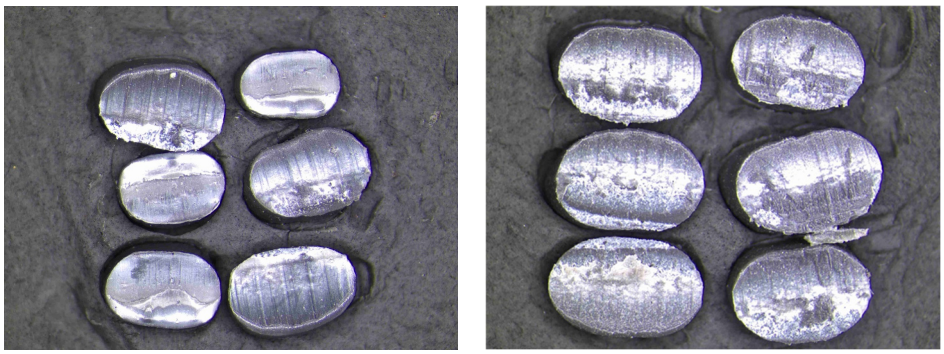
Values for PET 0.8 and PET 1.5 are not included because poor material properties prevented successful processing. PET 0.8 exhibited excessive fluidity and signs of degradation. At the same time, PET 1.5 showed very high viscosity and could only be processed at temperatures close to its degradation threshold, which did not allow sufficient residence time in the printer's screw extruder. High-temperature degradation led to excessive fluidification, making the material difficult to deposit properly.

3. Results and Discussion

The extrusion process for MPO flakes, with or without eggshell powder, did not show any operational issues. The process proceeded continuously and without interruptions, an aspect of relevance when considering a potential scale-up to industrial production. The material exiting the extruder appeared homogeneous and exhibited a smooth surface.

The plastic material, previously ground using a 4 mm screen, was properly fed into the extruder. The size of the grinder grid holes was then confirmed to be suitable for the application. The eggshell powder was introduced by means of a volumetric side feeder, positioned in the fourth heating zone, directly into the molten material, in order to limit excessive mechanical stress caused by friction between the extruder screws. Stereomi-

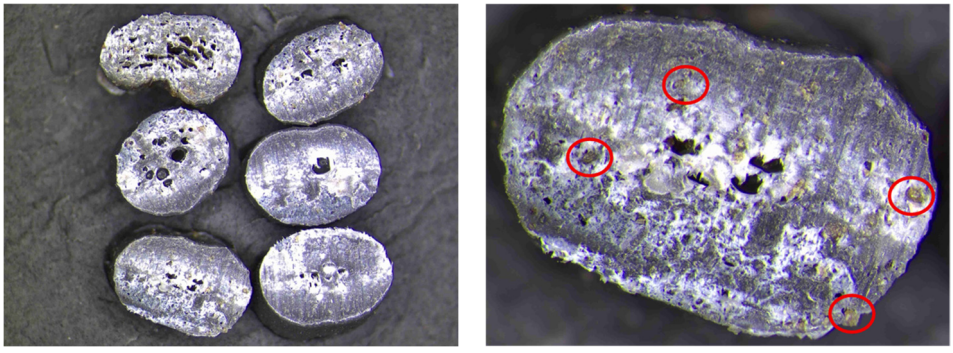
croscopic images of the plastic pellets obtained from the two extrusion processes show a uniform cross-section, without malformations or evident infused particles (Figure 7).



(**a**) (**b**)

Figure 7. Stereomicroscopy of Granules obtained from MPO flakes (**a**) and from MPO flakes with eggshell powder (**b**).

In contrast, the extrusion process with olive powder exhibited several critical issues, mainly related to the limited thermal stability of the organic filler. The processing temperatures, likely close to the tolerance limit of the material, combined with the mechanical stress generated by the extruder screws, may have caused degradation of the lignocellulosic filler, with consequent gas evolution. During extrusion, this phenomenon partially compromised the continuity of the process. The extrudate appeared swollen and was characterised by a highly rough surface. These conditions resulted in pellets with a cross-section showing pronounced porosity and poor material homogeneity. Stereomicroscopic analysis clearly highlights the presence of agglomerates attributable to lignocellulosic material that was not uniformly distributed or properly homogenised (Figure 8).



(**a**) (**b**)

Figure 8. Stereomicroscopy of granules obtained from MPO flakes with olive pit powder (**a**), zoom on lignocellulosic agglomerates highlighted with the red circles (**b**).

Possible operational strategies to improve the extrusion process of organic fillers include increasing the amount of compatibilising masterbatch and adding drying masterbatches, based on CaO, in mass percentages ranging from 1 to 2%.

The PET extrusion process did not show any particular issues related to material feeding into the extruder. PET was extruded either in its neat form or compounded with a chain extender. Joncryl® ADR-4400 is a multifunctional reactive polymer characterised by the presence of epoxy groups capable of reacting with the end groups of the polymer chains (Figure 9).

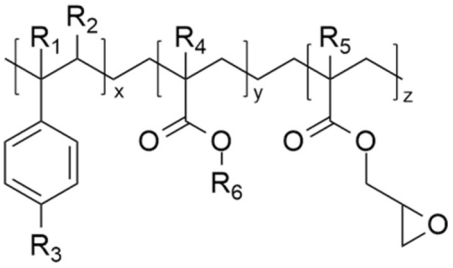
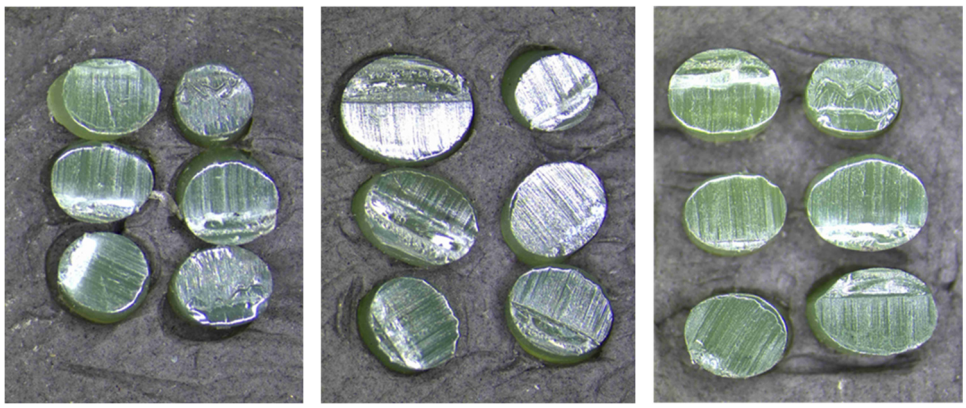


Figure 9. Chemical structure of Joncryl® ADR-4400.

Through this reaction mechanism, the additive promotes an increase in molecular weight and viscosity, leading to an improvement in the rheological properties of the treated material. During the extrusion process, Joncryl® ADR-4400 therefore plays a functional role in stabilising and controlling the processing conditions, ensuring improved overall processability. The effectiveness of the additive results in the production of a polymer with enhanced stability and performance during subsequent processing steps.

PET was extruded directly with the addition of the chain extender, and three different concentrations of Joncryl® ADR-4400 were tested to identify the optimal formulation. The PET 0.8 blend was found to be excessively fluid, making proper extrusion difficult. Conversely, the PET 1.5 blend exhibited very high viscosity and low melt strength, resulting in frequent filament breakage during extrusion. This behaviour can be attributed to an overdose of Joncryl® ADR-4400, which led to material starvation during processing. The PET 1 blend proved to be the optimal formulation, as the material exhibited appropriate viscosity and sufficient fluidity to allow for stable and continuous extrusion without interruptions. The resulting pellets appear as a glossy green material (Figure 10).



(**a**) (**b**) (**c**)

Figure 10. Stereomicroscopy of granules PET 0.8 (**a**), PET 1 (**b**), and PET 1.5 (**c**).

Tensile and flexural tests were performed on specimens produced by injection moulding and additive manufacturing. The results obtained from the two processing methods were compared for each material and further evaluated against commercially available products.

Commercial MPO materials are difficult to identify as directly comparable to our samples in the context of 3D printing, since their properties strongly depend on the quality of post-consumer waste, such as the quantity of PP or PE. Revet Replay 33K, a 50/50 PE–PP blend (Revet S.p.A., Pontedera (PI), Italy), with well-documented characteristics and a composition close to the formulation, was selected as a reference material only to see if the materials obtained in this work are better in characteristics with respect to this last commercial possibility. Regarding PET, the data were not obtained from processing

granules but were instead taken from values reported in the literature, given the extensive research activity in the field of R-PET.

For injection moulding, reference for tensile test was made to the results of a master's thesis in which the mechanical properties of various virgin and recycled PET packaging from different manufacturers were evaluated using type 1A injection-moulded tensile specimens and crystallinity between 50% and 60% [28]. The references for the bending tests on injection-moulded specimens were taken from the work of Celik, Y.; Shamsuyeva, M.; Endres, H.J [29] in which the injection moulding parameters and the relevant standards were consistent with those used in our tests.

For Additive Manufacturing, the reference for both tensile and flexural tests was from the work of Mishra, V., Ror, C.K., Negi, S. et al. [30], in which R-PET and V-PET were printed at 250, 260, and 270 °C, with 100% rectilinear infill at 0° and a 0.6 mm nozzle. For comparison, the values of the specimens printed at 260 °C were considered, corresponding to the printing temperature of our samples.

3.1. MPO

The mechanical characterisation, summarised in Tables 3 and 4, highlights significant differences between the four materials and between injection moulding and 3D printing for the investigated formulations of MPO blend.

Table 3. Tensile and flexural tests performed on injection-moulded MPO and Replay 33K.

Tensile tests			
	Tensile Modulus (MPa)	Yield strength (MPa)	Breaking deformation (%)
Replay 33K	1096.5 ± 20.02	23.16 ± 0.32	329 ± 25.21
MPO	1173.31 ± 38.40	26.46 ± 0.46	42.93 ± 4.49
MPO Olive	1391.52 ± 5.88	25.62 ± 0.20	10.87 ± 1.36
MPO Eggs	1301.04 ± 18.62	25.66 ± 0.28	146.65 ± 16.28

Flexural tests	
	Flexural Modulus (MPa)
Replay 33K	1105 ± 8.74
MPO	1120.21 ± 9.57
MPO Olive	1289.71 ± 17.45
MPO Eggs	1206.91 ± 4.18

From the analysis of the tensile test results (Table 3), significant differences in the mechanical behaviour of the three produced materials were observed. In terms of stiffness, the highest value of the elastic modulus was recorded for the MPO Olive sample (1391.52 ± 5.88 MPa), followed by MPO Eggs (1301.04 ± 18.62 MPa), while MPO exhibited the lowest value (1173.31 ± 38.40 MPa). These results indicate a more pronounced reinforcing effect for the Olive organic filler. This may be because the lignocellulosic filler could have a greater reinforcing effect than calcium carbonate due to its polymeric nature.

Despite the differences in elastic modulus, the yield stress values are very similar for all samples, ranging between approximately 25.6 and 26.5 MPa. This behaviour suggests that the addition of different fillers does not significantly affect the onset of plastic deformation but mainly influences the stiffness and post-yield mechanical response of the material.

Table 4. Tensile and flexural tests performed on 3D printed MPO and Replay 33K.

Tensile tests			
	Tensile Modulus (MPa)	Yield strength (MPa)	Breaking deformation (%)
Replay 33K	834.16 ± 47.58	15.97 ± 0.21	5.26 ± 1.45
MPO	1200.38 ± 65.82	24.22 ± 1.08	4.87 ± 0.37
MPO Olive	919.19 ± 43.14	12.47 ± 1.35	2.17 ± 0.31
MPO Eggs	1044.78	/	4.50 ± 0.81

Flexural tests	
	Flexural Modulus (MPa)
Replay 33K	975.46 ± 67.68
MPO	1276.86 ± 29.68
MPO Olive	942.40 ± 47.27
MPO Eggs	1296.35 ± 66.53

More pronounced differences emerge when considering the elongation at break, which highlights three distinct failure mechanisms:

In the case of MPO, a sharp fracture of the specimen was not observed; instead, progressive fibrillation occurred. As shown in Figure 11, the fracture surface exhibits a central cavity that fails first, followed by significant elongation of the outer region. This behaviour is characteristic of a ductile fracture mechanism, with a relatively high elongation at break (42.93 ± 4.49%).



Figure 11. MPO tensile test specimens at break.

The MPO Oliva sample, on the other hand, showed a very low elongation at break (10.87 ± 1.36%) and a clean, brittle fracture, as illustrated in Figure 12. This behaviour is likely due to a non-uniform dispersion of the organic filler within the polymer matrix, which may promote the formation of stress concentration sites, facilitating crack initiation and propagation.

For MPO Eggs, a fracture behaviour similar to that observed for MPO was found (Figure 13), but with an even more pronounced plastic deformation, as confirmed by the extremely high elongation at break value (146.65 ± 16.28%). The fracture surface suggests good matrix–filler adhesion and effective energy dissipation mechanisms, allowing the material to sustain large deformations before final failure.



Figure 12. MPO Olive tensile test specimens at break.



Figure 13. MPO Eggs tensile test specimens at break.

Overall, the results indicate that, although the yield stress and yield strain remain essentially unchanged, the type of filler plays a key role in determining the stiffness and, above all, the fracture behaviour of the material, leading to a transition from a more brittle response (MPO Olive) to a highly ductile one (MPO Eggs).

For Replay 33K, the tensile properties obtained by injection moulding are significantly higher than those achieved through additive manufacturing. In particular, the Tensile Modulus is markedly higher for injection-moulded samples compared to 3D-printed ones. A similar trend is observed for the yield strength, which decreases from 23.16 MPa for injection moulding to 15.97 MPa for 3D printing. Tensile strength further confirms this behaviour, with superior values for injection-moulded specimens (30.07 MPa) relative to additively manufactured ones (25.11 MPa). These results indicate that the mechanical performance of Replay 33K is strongly dependent on the processing route.

For MPO, the mechanical properties obtained via the two processing techniques are largely comparable. The Tensile Modulus shows very similar values, with a slight advantage for 3D-printed samples (1200.38 MPa) compared to injection-moulded ones (1173.31 MPa). Yield strength values are also close, while tensile strength is slightly higher for 3D-printed specimens. These findings suggest that the mechanical properties of MPO remain substantially unaffected by the manufacturing process, in contrast to Replay 33K, where the higher polypropylene content could play a key role in determining the final mechanical response.

In the case of MPO Eggs, the presence of calcium carbonate leads, as expected, to an increase in both tensile and flexural modulus, resulting in a stiffer and more resistant material compared to neat MPO. However, the Tensile Modulus of 3D-printed samples is lower than that of injection-moulded ones (1044.78 MPa versus 1301.04 MPa). A similar reduction

is observed for the yield strength. Conversely, tensile strength remains almost unchanged between the two processing routes (29.40 MPa for injection moulding and 28.45 MPa for 3D printing). Overall, the addition of calcium carbonate significantly enhances the elastic modulus while having a limited effect on yield strength, and the material retains a ductile fracture behaviour.

For MPO Olives, the comparison between injection moulding and additive manufacturing clearly highlights the superiority of injection moulding. The Tensile Modulus is substantially higher for injection-moulded samples (1391.52 MPa) compared to 3D-printed ones (919.19 MPa). Both yield strength and tensile strength are drastically reduced in 3D-printed specimens, decreasing from 25.62 MPa to 12.47 MPa and from 29.68 MPa to 21.09 MPa, respectively.

It is worth noting that all additively manufactured specimens exhibited brittle fracture behaviour, characterised by yield and tensile strength values that are practically overlapping.

Flexural tests further corroborated the tensile test results for Replay 33K and MPO Olives, showing consistent trends between the two loading modes. Conversely, for MPO and MPO Eggs, an opposite trend was observed, with injection-moulded samples exhibiting lower flexural properties compared to those obtained through additive manufacturing.

3.2. PET

Tables 5 and 6 summarise the results of the Tensile and Flexural tests performed on the PET specimens obtained both by injection moulding and 3D printing.

Table 5. Tensile and flexural tests performed on injection-moulded PET.

Tensile tests			
	Tensile Modulus (MPa)	Yield strength (MPa)	Breaking deformation (%)
PET 0.8	2254.28 ± 14.42	/	2.77 ± 0.87
PET 1	2176.50 ± 18.17	64.03 ± 0.61	187.24 ± 35.46
PET 1.5	2168.43 ± 14.42	61.28 ± 0.43	181.97 ± 10.04
Flexural tests			
	Flexural Modulus (MPa)		Breaking deformation (%)
PET 0.8	2651.53 ± 36.01		2.27 ± 0.44
PET 1	2312.49 ± 24.38		-
PET 1.5	2243.71 ± 30.62		-

Table 6. Tensile and flexural tests performed on 3D-printed PET.

Tensile test			
	Tensile Modulus (MPa)	Yield strength (MPa)	Breaking deformation (%)
PET 1	2656.98 ± 506.20	24.36 ± 9.43	1.02 ± 0.28
Flexural test			
	Flexural Modulus (MPa)		Breaking deformation (%)
PET 1	2480.09 ± 256.48		2.25 ± 0.12

Regarding the reference values of virgin PET under tensile testing, the elastic modulus was found to be 2236 MPa for injection-moulded specimens and 908.96 MPa for 3D-printed

ones. The yield strength in tension reached 53.5 MPa for injection moulding and 24.32 MPa for 3D printing. In flexural tests, the elastic modulus was consistent with tensile values, although a larger dispersion of results was observed. The maximum flexural strength was 67.5 MPa for injection moulding and 26.33 MPa for 3D printing.

For recycled PET, tensile tests showed an elastic modulus of 2068.42 MPa for injection-moulded specimens and 975.02 MPa for 3D-printed ones. The yield strength was 54.08 MPa for injection moulding and 19.27 MPa for 3D printing. In flexural tests, the elastic modulus differed from that obtained in tensile tests. This discrepancy can be attributed to the fact that the values were taken from different studies and to the significant variability of the physicochemical characteristics of recycled PET. The maximum flexural strength was 79.16 MPa for injection moulding and 14.92 MPa for 3D printing.

From the analysis of the tensile (ISO 527, 1BA) and flexural (ISO 178) test results, clear differences in the mechanical behaviour of PET formulations with different Joncryl® ADR-4400 contents can be identified, as well as the influence of the processing route.

For the injection-moulded materials, very similar Tensile Modulus values were obtained across all three PET formulations, a trend that is also confirmed by the flexural test results. Specifically, the Tensile Modulus was 2254.28 ± 14.42 MPa for PET 0.8, 2176.50 ± 18.17 MPa for PET 1, and 2168.43 ± 14.42 MPa for PET 1.5, indicating that increasing the Joncryl® ADR-4400 content beyond 1% does not lead to significant variations in stiffness. A similar trend was observed in flexure, where PET 0.8 exhibited the highest flexural modulus (2651.53 ± 36.01 MPa), followed by PET 1 (2312.49 ± 24.38 MPa) and PET 1.5% (2243.71 ± 30.62 MPa).

In terms of yield strength, PET 1 achieved the highest value (64.03 ± 0.61 MPa), slightly exceeding that of PET 1.5 (61.28 ± 0.43 MPa), suggesting the presence of an optimal chain extender concentration that maximises resistance to plastic deformation. This formulation also exhibited the highest maximum flexural strength (85.62 MPa). For PET 0.8, injection-moulding tests revealed a wider dispersion of mechanical results, indicating a less stable and more heterogeneous mechanical response.

A marked difference among the formulations is observed in terms of elongation at break. Both PET 1 and PET 1.5 display very high elongation at break values (187.24 ± 35.46% and 181.97 ± 10.04%, respectively), clearly indicating ductile behaviour with extensive plastic deformation prior to failure. In contrast, PET 0.8 shows a brittle mechanical response, characterised by a very low elongation at break (2.77 ± 0.87%) and the absence of a distinct yielding region. This brittle behaviour is further confirmed by flexural tests, in which PET 0.8 specimens fractured before reaching 5% of displacement, with a flexural strain at break of only 2.27 ± 0.44%.

Regarding additively manufactured PET, a different mechanical response was observed. Notably, the elastic modulus of PET 1 produced by 3D printing (2656.98 MPa) was even higher than that of the corresponding injection-moulded specimens, in contrast with trends commonly reported in the literature. However, this increase in stiffness was accompanied by a significant reduction in yield strength (24.36 MPa) and maximum flexural strength (59.66 MPa) compared to injection-moulded samples. Furthermore, 3D printing profoundly altered the fracture behaviour of the specimens, which shifted from ductile to brittle (Figure 14). This change is likely associated with insufficient control of pellet moisture content prior to processing, which is known to promote hydrolytic degradation of PET and premature failure during mechanical loading.

Overall, these results indicate that while injection moulding yields consistent mechanical properties across different PET formulations, the Joncryl® ADR-4400 content strongly affects the balance between stiffness and ductility. A Joncryl® ADR-4400 content of at least 1% appears necessary to promote ductile behaviour, whereas lower concentrations increase

stiffness at the expense of fracture resistance. Additive manufacturing, although capable of achieving high stiffness in specific formulations, significantly compromises strength and ductility, highlighting the critical role of processing conditions—particularly moisture control—in determining the final mechanical performance of PET-based materials.



(**a**) (**b**)

Figure 14. Injection-moulded PET 1 (**a**) and 3D-printed PET 1 (**b**) tensile test specimens at break.

4. Conclusions

The comparative analysis between injection moulding and additive manufacturing highlighted distinct behaviours depending on the polyolefin formulation. Replay 33K, derived from household-recovered plastic waste, showed superior performance when processed by injection moulding, with higher Tensile Modulus, yield strength, and tensile strength compared to 3D-printed specimens.

MPO exhibited mechanical properties largely unaffected by the processing route, with 3D printing in some cases—such as tensile strength—yielding slightly better values. MPO Eggs displayed an intermediate behaviour, with a higher Tensile Modulus in 3D-printed samples but superior yield strength in injection-moulded ones. Conversely, MPO Olives confirmed the clear superiority of injection moulding, as 3D-printed specimens suffered significant performance losses and brittle fractures.

For PET-based materials, also obtained from marine recovery, the addition of a chain extender allowed the elastic modulus to remain comparable to that of virgin PET, while yield strength increased consistently with literature values. The best performance was observed for the formulation containing 1% Joncryl® ADR-4400. Flexural tests confirmed these trends, except for the elastic modulus, which showed a countertrend: 3D-printed specimens exhibited lower values compared to their injection-moulded counterparts.

Given that the materials tested were recovered directly from the marine environment, these findings are particularly relevant. They demonstrate that, even starting from an alternative recycling pathway compared to the conventional solid waste stream, it is possible to achieve competitive mechanical performance, in some cases comparable to those of recycled materials already available on the market. Further chemical analyses, currently in progress, will provide a more complete understanding of the mechanisms involved and help assess the full application potential of this recycling approach.

In parallel, work currently underway will determine the circular economy viability of the model, in order to determine the extent to which the proposed technical solutions can be replicated elsewhere and scaled up to constitute a realistic alternative to the take-make-waste linear economy.

https://doi.org/10.3390/engproc2026131029

Author Contributions: Investigation, A.S., P.L.-M., M.M. and S.B.; Data curation, A.B., M.A. and M.C.; Writing—original draft preparation, A.S.; Writing—review and editing, A.S., M.F., M.A., M.C., S.B., E.G. and C.C.; Supervision, M.F., M.A., M.C., S.B., E.G. and C.C.; Project administration, M.A., M.C., S.B., E.G. and C.C.; Funding acquisition, M.F. All authors have read and agreed to the published version of the manuscript.

Funding: This research was funded by the Interreg Italy–France Maritime Programme 2021–2027 (PLASTRON Project), grant number €1,467,718.82 (ERDF Check the website: https://interreg-marittimo.eu/web/plastron accessed on 30 March 2026).

Institutional Review Board Statement: Not applicable.

Informed Consent Statement: Not applicable.

Data Availability Statement: The original contributions presented in this study are included in the article. Further inquiries can be directed to the corresponding authors.

Acknowledgments: We thank the associations Fondali Puliti, Spazzapnea, Legambiente, and the Coop Pescatori di S. M. Ligure for providing the materials. We also thank the company Revet S.p.A. for making the equipment and process expertise available. We also thank Pietro Carli of Revet S.p.A.

Conflicts of Interest: Author S.B. was employed by the company Revet S.p.A. The remaining authors declare that the research was conducted in the absence of any commercial or financial relationships that could be construed as a potential conflict of interest.

References

1. STAP. *Marine Debris as a Global Environmental Problem: Introducing a Solutions Based Framework Focused on Plastic. A STAP Information Document*; Global Environment Facility: Washington, DC, USA, 2011.
2. UNEP. *Limiti Legali per la Plastica Monouso e le Microplastiche: Un Rapporto Globale*; UNEP: Nairobi, Kenya, 2019.
3. Issifu, I.; Sumaila, U.R. A Review of the Production, Recycling and Management of Marine Plastic Pollution. *J. Mar. Sci. Eng.* **2020**, *8*, 945. [CrossRef]
4. Veksha, A.; Ahamed, A.; Wu, X.Y.; Liang, L.; Chan, W.P.; Giannis, A.; Lisak, G. Technical and environmental assessment of laboratory scale approach for sustainable management of marine plastic litter. *J. Hazard. Mater.* **2022**, *421*, 126717. [CrossRef] [PubMed]
5. Silva, D.; Garrido, J.; Lekube, B.; Arrillaga, A. On-board and port 3D printing to promote a maritime plastic circular economy. *J. Clean. Prod.* **2023**, *407*, 137151. [CrossRef]
6. OECD. *Global Plastics Outlook*; OECD: Paris, France, 2022. [CrossRef]
7. Beaumont, N.J.; Aanesen, M.; Austen, M.C.; Börger, T.; Clark, J.R.; Cole, M.; Hooper, T.; Lindeque, P.K.; Pascoe, C.; Wyles, K.J. Global ecological, social and economic impacts of marine plastic. *Mar. Pollut. Bull.* **2019**, *142*, 189–195. [CrossRef]
8. Curmi, A.; Rochman, A. Screw extrusion fused granulate Fabrication: Trends, materials, extruder classification and future development. *Polymer* **2025**, *330*, 128459. [CrossRef]
9. Fontana, L.; Giubilini, A.; Arrigo, R.; Malucelli, G.; Minetola, P. Characterization of 3D Printed Polylactic Acid by Fused Granular Fabrication through Printing Accuracy, Porosity, Thermal and Mechanical Analyses. *Polymers* **2022**, *14*, 3530. [CrossRef]
10. Frascio, M.; Bergonzi, L.; Jilich, M.; Moroni, F.; Avalle, M.; Pirondi, A.; Monti, M.; Vettori, M. Additive manufacturing process parameter influence on mechanical strength of adhesive joints, preliminary activities. *Acta Polytech. CTU Proc.* **2019**, *25*, 41–47. [CrossRef]
11. Frascio, M.; Zafferani, A.; Monti, M.; Avalle, M. Investigating enhanced interfacial adhesion in multi-material filament 3D printing: A comparative study of t and Mickey Mouse geometries. *Prog. Addit. Manuf.* **2024**, *9*, 2113–2122. [CrossRef]
12. Avalle, M.; Monti, M.; Frascio, M. Modeling the strength of laminated parts made by fused filament fabrication additive manufacturing. *Proc. Inst. Mech. Eng. C J. Mech. Eng. Sci.* **2023**, 095440622311614. [CrossRef]
13. Avalle, M.; Frascio, M.; Monti, M. An improved model to describe the repeated loading-unloading in compression of cellular materials. *Procedia Struct. Integr.* **2018**, *12*, 19–31. [CrossRef]
14. Romani, A.; Levi, M. Large-Format Material Extrusion Additive Manufacturing for Circular Economy Practices: A Focus on Product Applications with Materials from Recycled Plastics and Biomass Waste. *Sustainability* **2024**, *16*, 7966. [CrossRef]
15. Sabai, M.M.; Cox, M.G.D.M.; Mato, R.R.; Egmond, E.L.C.; Lichtenberg, J.J.N. Concrete block production from construction and demolition waste in Tanzania. *Resour. Conserv. Recycl.* **2013**, *72*, 9–19. [CrossRef]

16. Kaynak, B.; Spoerk, M.; Shirole, A.; Ziegler, W.; Sapkota, J. Polypropylene/Cellulose Composites for Material Extrusion Additive Manufacturing. *Macromol. Mater. Eng.* **2018**, *303*, 1800037. [CrossRef]
17. Cañado, N.; Lizundia, E.; Akizu-Gardoki, O.; Minguez, R.; Lekube, B.; Arrillaga, A.; Iturrondobeitia, M. 3D printing to enable the reuse of marine plastic waste with reduced environmental impacts. *J. Ind. Ecol.* **2022**, *26*, 2092–2107. [CrossRef]
18. Maldonado-García, B.; Pal, A.K.; Misra, M.; Gregori, S.; Mohanty, A.K. Sustainable 3D printed composites from recycled ocean plastics and pyrolyzed soy-hulls: Optimization of printing parameters, performance studies and prototypes development. *Compos. Part C Open Access* **2021**, *6*, 100197. [CrossRef]
19. Geissdoerfer, M.; Savaget, P.; Bocken, N.M.P.; Hultink, E.J. The Circular Economy—A new sustainability paradigm? *J. Clean. Prod.* **2017**, *143*, 757–768. [CrossRef]
20. Ragauskaitė, D.; Šlinkšienė, R. Influence of Urea on Organic Bulk Fertilizer of Spent Coffee Grounds and Green Algae *Chlorella* sp. Biomass. *Sustainability* **2022**, *14*, 1261. [CrossRef]
21. Bergonzi, L.; Pirondi, A.; Moroni, F.; Frascio, M.; Avalle, M. A study on additive manufacturing build parameters as bonded joint design factors. *J. Adhes.* **2024**, *100*, 576–605. [CrossRef]
22. Merino, P.L.; Charlier, C.; Guerci, E. Governing Plastic as Commons: Polycentric and Adaptive Pathways to a Circular Economy in the Mediterranean. *Innovations* **2025**, *hors-série*, 72. [CrossRef]
23. Saechtling, H. *Manuale Delle Materie Plastiche*, 10th ed.; Tecniche Nuove: Milan, Italy, 2006.
24. Ojeda, T.; Freitas, A.; Birck, K.; Dalmolin, E.; Jacques, R.; Bento, F.; Camargo, F. Degradability of linear polyolefins under natural weathering. *Polym. Degrad. Stab.* **2011**, *96*, 703–707. [CrossRef]
25. Toro, P.; Quijada, R.; Yazdani-Pedram, M.; Arias, J.L. Eggshell, a new bio-filler for polypropylene composites. *Mater. Lett.* **2007**, *61*, 4347–4350. [CrossRef]
26. Elgharbawy, A.S.; Ali, R.M. A comprehensive review of the polyolefin composites and their properties. *Heliyon* **2022**, *8*, e09932. [CrossRef]
27. Brooks, D.W.; Giles, G.A. (Eds.) *PET Packaging Technology*; Sheffield Academic Press: Sheffield, UK, 2002.
28. Lund, A. *Material Properties of Recycled PET in Beverage Containers*; KTH, School of Chemistry, Biotechnology and Environmental Engineering: Stockholm, Sweden, 2021.
29. Celik, Y.; Shamsuyeva, M.; Endres, H.J. Thermal and Mechanical Properties of the Recycled and Virgin PET—Part, I. *Polymers* **2022**, *14*, 1326. [CrossRef]
30. Mishra, V.; Ror, C.K.; Negi, S.; Veeman, D. Recycling PET Waste into Functional 3D Printing Material: Effect of Printing Temperature on Physio-mechanical Properties of PET Parts. *J. Mater. Eng. Perform.* **2025**, *34*, 26778–26790. [CrossRef]

Disclaimer/Publisher's Note: The statements, opinions and data contained in all publications are solely those of the individual author(s) and contributor(s) and not of MDPI and/or the editor(s). MDPI and/or the editor(s) disclaim responsibility for any injury to people or property resulting from any ideas, methods, instructions or products referred to in the content.